

# ProSpect: Expanded Conditioning for the Personalization of Attribute-aware Image Generation

Yuxin Zhang Weiming Dong  
MAIS, Institute of Automation, CAS  
China

Fan Tang  
ICT, CAS  
China

Nisha Huang  
School of Artificial Intelligence, UCAS  
China

Haibin Huang Chongyang Ma  
Kuaishou Technology  
China

Tong-Yee Lee  
National Cheng-Kung University  
Taiwan

Oliver Deussen  
University of Konstanz  
Germany

Changsheng Xu  
MAIS, Institute of Automation, CAS  
China

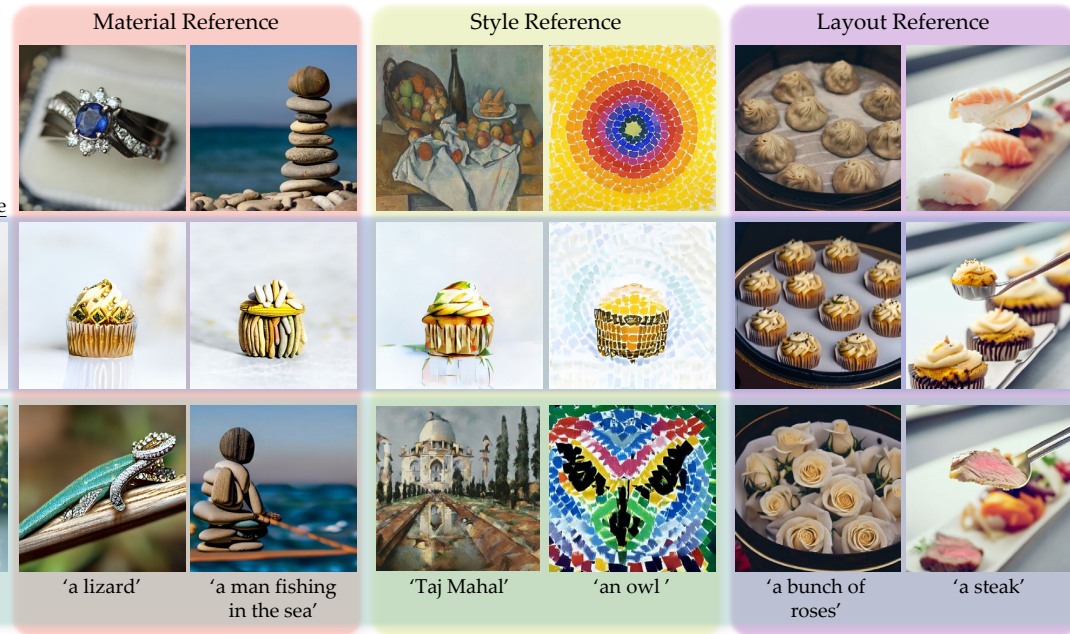


Figure 1: Attribute-aware image generation results using *ProSpect*. Given only a single input image or text prompts, our method can accurately control the visual attributes such as material, style, content, and layout to generate a new image with the learned textual conditionings.

## ABSTRACT

Personalizing generative models offers a way to guide image generation with user-provided references. Current personalization methods can invert an object or concept into the textual conditioning space and compose new natural sentences for text-to-image diffusion models. However, representing and editing specific visual attributes like material, style, layout, etc. remains a challenge, leading to a lack of disentanglement and editability. To address this, we propose a novel approach that leverages the step-by-step generation process of diffusion models, which generate images from low-to high-frequency information, providing a new perspective on representing, generating, and editing images. We develop Prompt

Spectrum Space  $\mathcal{P}^*$ , an expanded textual conditioning space, and a new image representation method called *ProSpect*. *ProSpect* represents an image as a collection of inverted textual token embeddings encoded from per-stage prompts, where each prompt corresponds to a specific generation stage (i.e., a group of consecutive steps) of the diffusion model. Experimental results demonstrate that  $\mathcal{P}^*$  and *ProSpect* offer stronger disentanglement and controllability compared to existing methods. We apply *ProSpect* in various personalized attribute-aware image generation applications, such as image/text-guided material/style/layout transfer/editing, achieving previously unattainable results with a single image input without fine-tuning the diffusion models. Codes are available at <https://github.com/zyxElsa/ProSpect>.

## CCS CONCEPTS

- Computing methodologies → Image processing.

## KEYWORDS

Image generation, diffusion models, personalizing editing

## 1 INTRODUCTION

If we consider photography and painting as visual languages, we can understand that each image encapsulates a unique perspective or way of seeing. By harnessing the power of pre-trained diffusion models designed for text-to-image generation, we gain a versatile method for influencing the synthesis process using natural language commands. The utilization of these advanced generative models not only allows for the creation of realistic and diverse images but also enables users to personalize the output according to their visual preferences. Recent personalization methods [28, 48, 64, 87] learn the textual conditioning of a common concept (or item) within a set of images, and then use text to create new scenarios that incorporate that concept. However, representing specific visual attributes within a specific image remains a challenging problem for these concept-level personalization methods.

We believe that each visual attribute (e.g., style, material, layout, etc.) within an image possesses its unique features. Attribute-aware image generation, therefore, involves the disentanglement, representation, and recombination of these visual attributes to guide image synthesis and editing. The primary challenge lies in disentangling the specific attributes within a single image, as they often appear in combination. Additionally, recombining the attributes without causing conflicts or distortions is difficult when performing image attribute transfer task.

By projecting image references into conditioned textual space (defined as  $\mathcal{P}$  [28], Fig. 2(a)), text-to-image generation methods could conduct concept-level image editing. However, generating single textual embedding across all diffusion steps and U-Net structure limits the ability for visual attribute disentanglement. In line with Gal et al. [28], Voynov et al. [97] observed that the shallow layers of denoising U-Net structures within diffusion models tend to generate colors and materials, while deep layers provide semantic guidance. In this paper, we conduct a detailed analysis of how the textual-conditioning influences the diffusion models' generation process. Various visualizations reveal that diffusion models generate images in the order of “*layout* → *content* → *material/style*”. Further analysis reveals that the generation order in a diffusion model is due to the frequency of the corresponding attribute's signal, which progresses from low to high. This insight paves the way for obtaining better disentanglement of visual attributes in diffusion models.

Inspired by the observation, we introduce Prompt Spectrum Space  $\mathcal{P}^*$  (see Fig. 2(c)), an expanded conditioning space of  $\mathcal{P}$  that provides a new insight on the diffusion generation process from the perspective of *steps*. Instead of treating all diffusion steps as a whole, we consider several groups of consecutive steps as different generation stages. Each stage corresponds to a unique textual condition  $p_i$ . We further propose a novel textual inversion method called Prompt Spectrum Inversion (*ProSpect*), which learns token embeddings  $P$  in  $\mathcal{P}^*$  from a single image. Unlike previous methods that

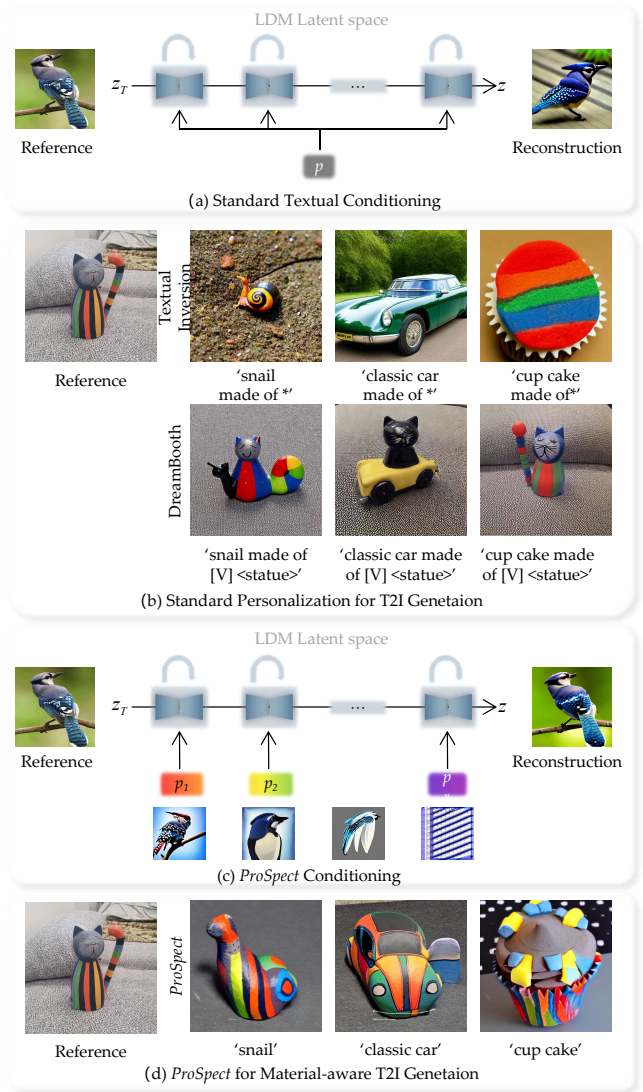


**Figure 2: Differences between (a) standard textual conditioning  $\mathcal{P}$  and (c) the proposed prompt spectrum conditioning  $\mathcal{P}^*$ .** Instead of learning global textual conditioning for the whole diffusion process, *ProSpect* obtains a set of different token embeddings delivered from different denoising stages. Textual Inversion [28] loses most of the fidelity. Compared with DreamBooth [87] that generates cat-like objects in the images, *ProSpect* can separate content and material, and is more fit for attribute-aware T2I image generation.

consider the concept or image as a whole, *ProSpect* provides a new way to represent an image in the perspective of frequency, which improves flexibility and editability. Various visual attributes can be separated from  $P$ , enabling attribute-aware generation. Specifically, we group the textual token embeddings  $p_i$  into three classes: material/style (high-frequency), content (medium-frequency), and layout (low-frequency). By replacing them with embeddings of

other images, we can achieve attribute transfer, as shown in the 2<sup>nd</sup> row of Fig. 1. *ProSpect* can transfer multiple attributes from a personalized image, including material, style, content, and layout, to new images. Compared to previous personalization approaches, our method offers greater transferability of diverse image visual attributes. Notably, in the context of attribute-aware image-to-text generation tasks, *ProSpect* demonstrates superior editability and fidelity, achieving results that were previously difficult to obtain, as shown in the 3<sup>rd</sup> row of Fig. 1. Figs. 2(b) and 2(d) show the differences between the standard personalization method Textual Inversion [28], DreamBooth [87] and *ProSpect* applying to material controlling tasks. Textual Inversion loses most of the fidelity. Due to the lack of separation of content and material, DreamBooth tends to generate cat-like objects in each image. *ProSpect* separates the content and material in the learning and conditioning process and can generate a new image that is little related to the content of the reference image. Extensive experiments and evaluations demonstrate the effectiveness of  $\mathcal{P}^*$  and *ProSpect*. Our contributions are:

- We introduce a novel prompt spectrum Space  $\mathcal{P}^*$  that enables the disentanglement of visual attributes from a single image. We also reveal that the diffusion model’s generation process is dependent on the image signal frequency.
- We present Spectrum Textual Inversion method (*ProSpect*), a novel image representation method that offers better controllability and flexibility when processing image visual attributes.
- Experimental results demonstrate the effectiveness of *ProSpect* in various attribute-aware image generation tasks.

## 2 RELATED WORK

*Text-guided image synthesis.* Generative Adversarial Network (GAN)-based architecture [32] was widely used in the text-to-image models, which were trained on large sets of paired image-caption data [69, 93, 102, 107, 110]. However, GANs have a tendency to suffer from mode collapse, and their training at scale can be challenging [10, 41]. Auto-regressive models [27, 84, 106] were inspired by the success of language models and approached the task of image generation by treating images as word sequences in a discrete latent space [26]. This scheme allowed for text guidance during generation through conditioning on text-prefix or using text-to-image similarity models [21, 30, 65] at test-time optimization. Recently, diffusion models [22, 75] have emerged as the forefront of image generation. These models have led to significant advancements in text-to-image synthesis, achieving more natural results with impressive diversity and fidelity [8, 14, 46, 74, 83, 85, 88].

*Personalization of generative models.* The personalization of the text-to-image generation model is the task of generating personalized content on the pre-trained generation model using prompt learning, model fine-tuning, etc. The task aims to learn the textual conditioning of a personalized concept from user-provided images and guide the generation of new images containing the concept. Gal *et al.* [28] present a textual inversion method to find a new pseudo-word to describe the visual concept of a specific object or artistic style in the embedding space of a fixed text-to-image model. They use optimization-based methods to directly optimize the embedding of the concept. Gal *et al.* [29] further design an encoder for fast

personalization on a single image. They train a word-embedding encoder to predict a new pseudo-word that best describes the input concept, and introduce weight offsets to specialize the text-to-image model to the target domain. Li *et al.* [68] invert the real image to the value linear mapping network input in cross-attention layers while freezing the key linear mapping network input with user-provided textual embedding, facilitating learning of initial attention maps and an estimated path for reconstructing the real image. Ruiz *et al.* [87] implant a subject into the output domain of a text-to-image diffusion model to synthesize it in novel views with a unique identifier. Their inversion method is based on the fine-tuning of diffusion models, which requires high computational resources. Zhang *et al.* [108] proposed an attention-based inversion method InST, which can efficiently obtain textual conditioning that describes the whole appearance of a single image without fine-tuning. Kumari *et al.* [63] propose Custom Diffusion, which needs to optimize a few parameters in the text-to-image conditioning mechanism and can jointly train for multiple concepts or combine multiple fine-tuned models. Huang *et al.* [48] propose ReVersion for the Relation Inversion task, which aims to learn a specific relation from a handful user-provided images. Wen *et al.* [98] introduce the concept of hard prompts that use hand-crafted sequences of interpretable tokens to elicit model behaviors and introduce an approach to robustly optimize hard text prompts through efficient gradient-based optimization. Voynov *et al.* [97] introduce an Extended Textual Conditioning space  $\mathcal{P}^+$  that consists of multiple textual conditions, derived from per-layer prompts, each corresponding to a layer of the denoising U-net of the diffusion model. They introduce Extended Textual Inversion (XTI), where the images are inverted into  $\mathcal{P}^+$ , and represented by per-layer tokens. Tewel *et al.* [94] introduce Perfusion, a new mechanism that “locks” new concepts’ cross-attention keys to their superordinate category, and a gated rank-1 approach to control the influence of a learned concept during inference time and to combine multiple concepts. Most of the aforementioned methods necessitate an image set (three to five) or fine-tuning the model, and they aim to learn a single concept in the image or represent the overall appearance of the image. In contrast, our approach addresses the challenges of obtaining multiple visual attributes from a single image, involving the disentanglement, representation, and recombination of visual attributes.

*Text-based image editing.* A variety of text-based editing methods [9, 78, 89] have emerged with the development of powerful multi-modal models. Enabled by diffusion models, approaches of different applications are developed, such as single-image editing [11, 45, 51, 71, 72, 96, 101, 109], style transfer [47, 50, 104] and inpainting [7, 70, 103]. The Composer approach, proposed by Huang *et al.* [43], is most relevant to our work. This approach introduces a generation paradigm that enables control over output image features while preserving synthesis quality and model creativity through decomposing images into representative factors (e.g., spatial layout, palette) and training a diffusion model using these factors as conditions for recombination. However, they rely on external professional models to obtain image attributes, such as an edge detection model for contour extraction, a pre-trained segmentation model for instance mask extraction, etc. In contrast,

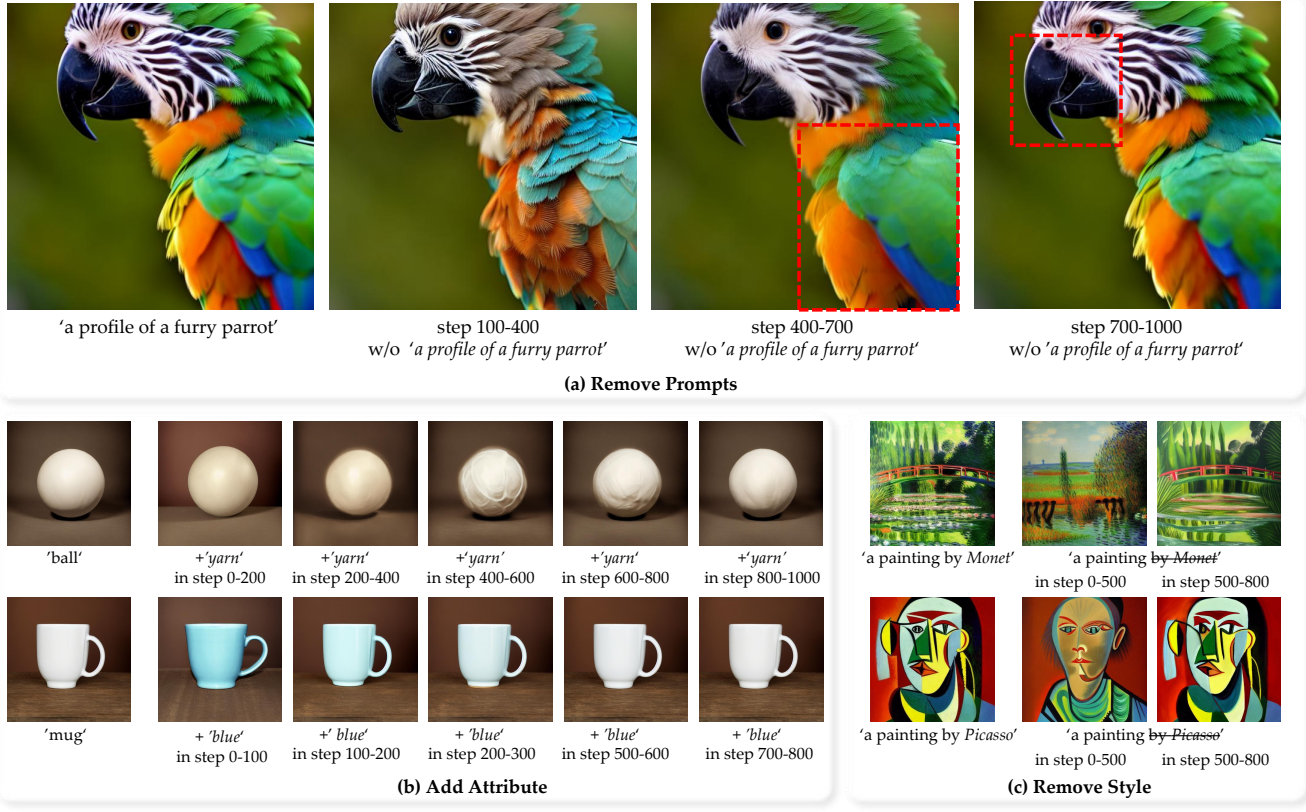


**Figure 3: Experimental results showing that different attributes exist at different steps. (a) Results of removing prompts “a profile of a furry parrot” of different steps. (b) Results of adding material attribute “yarn” and color attribute “blue”. (c) Results of removing style attribute “Monet” and “Picasso”.**

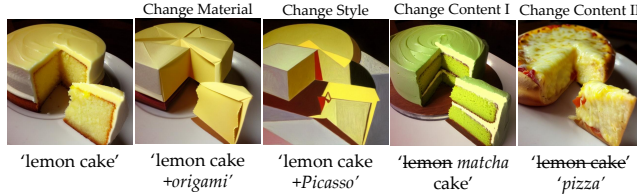


**Figure 4: The prompt editing results. By changing the prompts conditioning on different diffusion stages, and keeping the layout-related prompts unchanged, the effect of prompt-to-prompt editing can be achieved.**

we exclusively use the pre-trained diffusion model to acquire the representation of corresponding attributes from the image.

### 3 METHOD

To illustrate our motivation, we start by analyzing the attribute distribution of diffusion models using text-guided image generation results. We aim to obtain multiple visual attributes from a single image, thus we need to learn the range of the steps in which different attributes are generated in the model. Therefore, removing textual

conditions from some generation steps, or adding different types of textual conditions to some steps, can help us understand intuitively.

Fig. 3 shows the results of removing or adding attributes at different diffusion stages. In Fig. 3(a), removing a certain phase “a profile of a furry parrot” in some steps will cause specific changes to the generated image. Removing step 100-400 significantly changes the parrot’s appearance, but the new image retains the details and feather layering. Removing step 400-700 reduces the layering of the parrot’s feathers. Removing step 700-1000 blurs the parrot’s fur and the luster of the beak is gone, while it can retain a similar overall appearance to the original image. Fig. 3(b) demonstrates the effect of adding an attribute in a specific stage. In the 1<sup>st</sup> row, the sphere’s appearance remains unchanged when injected the added concept “yarn” in step 0-200, but the background layout and colors are different, and adding it in step 200-400 blurs the sphere’s outline. Injecting “yarn” in step 400-600 and step 600-800 produces a more distinct texture. Adding “yarn” in step 800-1000 creates a woolen texture on the sphere and reduces its reflection. The 2<sup>nd</sup> row shows that the diffusion model is color-sensitive only at certain stages. Fig. 3(c) shows the style removal results of impressionist Claude Monet and abstract painter Pablo Picasso. We removed their names

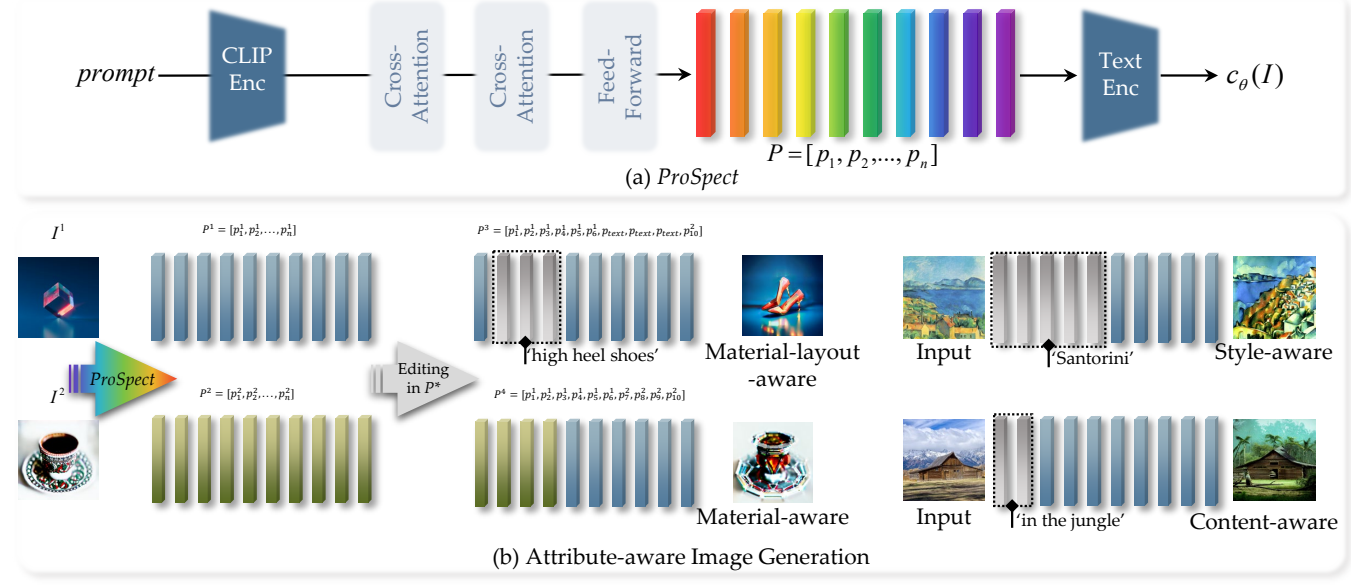


Figure 5: (a) The pipeline of *ProSpect*, which learns a set of token embeddings  $P = [p_1, p_2, \dots, p_n]$ . (b) Illustrations for various attribute-aware image generation.

at different stages, i.e., using only “*a painting*” to guide the generation. Removing the style in *step 500-800* has little effect on the *Picasso*-guided painting, but the *Monet*-guided painting loses its brushstrokes. Conversely, removing *step 0-500* changes the content of the paintings guided by “*Monet*”, but the style is maintained, while the image guided by “*Picasso*” loses its style. We recommend zooming in to see *Monet*’s experimental results better. In conclusion, the initial generation stages of the diffusion model tend to generate overall layout and color, the middle stages tend to generate structured appearances, and the final stages tend to generate detailed textures.

Based on the above observations, we can edit the results by changing the material, style, and content while keeping the layout unchanged just by changing the prompts that act on different steps. As shown in Fig. 4, keeping the prompt “*lemon cake*” condition in the initial stages, the image can be edited into different appearances. Similar visual effects can also be seen in prompt-to-prompt [39], they introduce a method that locks the corresponding attention maps.

### 3.1 Prompt Spectrum Space

We use stable Diffusion [85] as the generative backbone, which is built in the framework as the Latent Diffusion Model (LDM) [85]. LDM is a diffusion probability model that generates images by gradually denoising them.

Voynov et al. [97] introduce a textual-conditioning space  $\mathcal{P}$ , which refers to the token embeddings sent to the text encoder of a diffusion model. After undergoing CLIP encoding, each token is used as the codebook key to obtain its corresponding embedding in  $\mathcal{P}$ , corresponding to each word. These embeddings are concatenated and fed into the text encoder, which outputs a suitable conditional

encoding for the diffusion model. This encoding is then injected layer by layer into the U-Net model, which denoises a noise image.

Diffusion and denoising within an LDM typically take 1000 steps, and the text conditions the model step by step. Previously, the process of the textual conditions acting on the diffusion model is regarded as a whole. In this work, we treat them as different procedures. Specifically, we divide the 1000 steps of conditioning into ten stages averagely. Each stage corresponds to a unique textual condition. The collection of textual conditions reside in the CLIP [82] text-image space, their size is set to  $n \times 1 \times 768$  ( $n = 10$  denotes the number of the stages). This way of division is designed to keep a balance between speed and subdivision.

We refer to the expanded space as the *Prompt Spectrum Space*, denoted as  $\mathcal{P}^*$ . An illustration of how  $\mathcal{P}$  and  $\mathcal{P}^*$  interact with text and diffusion models is shown in Figs. 2(a) and 2(b). Thus,  $\mathcal{P}^*$  is defined as:

$$\mathcal{P}^* = \{p_1, p_2, \dots, p_n\}, \quad (1)$$

where  $p_i$  represents the token embedding corresponding to the conditional prompt of  $i$  in the diffusion model stage.

### 3.2 Spectrum Textual Inversion

Text Inversion (TI) aims to obtain the textual token embedding of an image set within the  $\mathcal{P}$  space. Our goal is to extend TI to  $\mathcal{P}^*$  to extract a set of textual token embeddings from an input image. To achieve this, we present *ProSpect*, a method that maps an image to a collection of corresponding textual token embeddings. The TI loss of LDM in  $\mathcal{P}$  space is formulated as:

$$\mathcal{L}_{TI} = \mathbb{E}_{z, t, p} [\|\epsilon - \epsilon_\theta(z, t, p_\theta)\|_2^2], \quad (2)$$

where  $p_\theta$  is a learnable vector denoting the token embedding and,  $z \sim E(x), \epsilon \sim \mathcal{N}(0, 1)$ . Similarly, the *ProSpect* loss of LDM in  $\mathcal{P}^*$

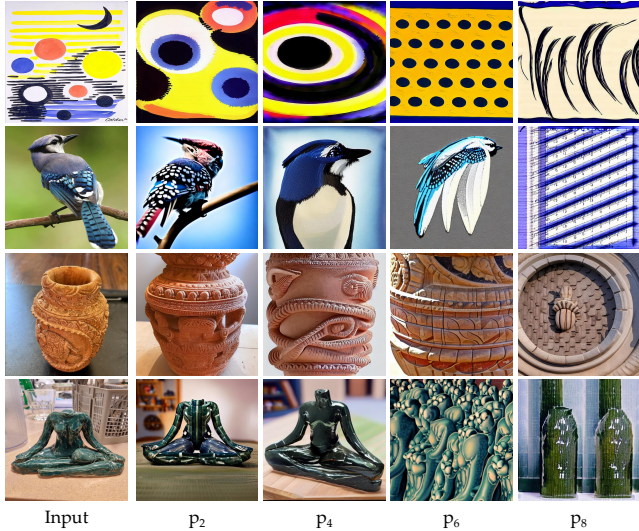


Figure 6: The visualization results of token embeddings  $p_i$  obtained by *ProSpect*. The results show that the initial generation step of the diffusion model is sensitive to structural information (e.g., bird’s pose, pot’s shape). As the number of steps increases, the obtained  $p_i$  gradually captures detailed information (e.g., the sideways head of the bird → bird’s wing → the texture of the bird’s feathers).

space is formulated as:

$$\mathcal{L}_{PS} = \mathbb{E}_{z,t,p} \left[ \|\epsilon - \epsilon_\theta(z_t, t, p_i)\|_2^2 \right], \quad (3)$$

where  $p_i = P(t)$  is a learnable vector represents the token embedding of stage  $i$ , and  $P = [p_1, p_2, \dots, p_n]$  is the set of textual token embeddings in  $\mathcal{P}^*$  space.

Fig. 5(a) illustrates the network structure. The input prompt is fed into the CLIP text encoder, which generates the textual token embedding. The token embedding is fed to the attention modules and a feed-forward module. Optimizing attention and feed-forward networks by  $\mathcal{L}_{PS}$  loss, the final  $p_i$  is obtained. Dropout is applied to prevent overfitting and the rate is set to 0.1.

## 4 ANALYSIS OF $\mathcal{P}^*$

### 4.1 Image Attribute Visualization

We visualize the token embedding  $p_i$  obtained by *ProSpect* by using it as the condition of the entire stage of the diffusion model, i.e.,  $p_{1:10} = p_i$ . Fig. 6 shows the visualization results of  $p_i$  corresponding to the four stages. It can be seen that the diffusion model gives different penalties to token embeddings  $p_i$  at different stages to reconstruct the given image. The token embeddings that are conditioned on the initial stages are optimized to denote structure information, and then gradually represent detailed information as the generation steps increase. For instance,  $p_2$  tends to represent the layout or content, while  $p_8$  tends to express the textures or brushstrokes. The results strongly indicate that different generation tendencies exist in different stages of the diffusion model.

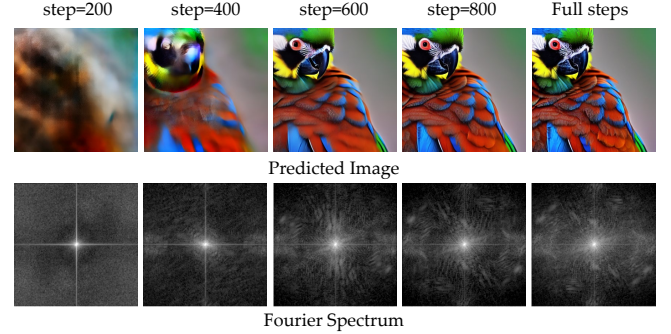


Figure 7: The 1<sup>st</sup> row shows the predicted image obtained at different denoising steps with the text prompt “*a close-up photo of a parrot*”. The 2<sup>nd</sup> row showcases the Fourier spectrum of each predicted image. As the denoising process progresses, the high-frequency information contained in the diffusion model’s predicted image gradually increases. We enhanced the contrast of the Fourier spectrum to improve its clarity.

### 4.2 Analysis and Explanation

The experimental results demonstrate that the diffusion model generates images in the order of “*layout* → *content* → *material/style*”. A similar phenomenon has been observed in convolutional networks. Voynov *et al.* [97] noted that the U-Net structure of the diffusion model has similar properties, with the shallow layer tending to generate texture and color and the deep layer generating semantic information. It is important to note that the deep receptive field size of U-Net is larger than the shallow receptive field size, making the hierarchical attribute distribution easy to comprehend. However, this size difference does not exist between steps of the diffusion model, as the latent size is uniform across different stages. Therefore, further analysis is necessary to understand the attribute tendency of different generation stages.

The diffusion model continuously adds noise to the initial data distribution  $x_0$  and finally makes the data distribution into independent Gaussian distributions. The forward diffusion process is defined as:

$$q(x_t | x_{t-1}) = \mathcal{N} \left( x_t; \sqrt{1 - \beta_t} x_{t-1}, \beta_t I \right),$$

$$q(x_{1:T} | x_0) = \prod_{t=1}^T q(x_t | x_{t-1}). \quad (4)$$

$q(x_t)$  can be derived by reparameterization:

$$x_t = \sqrt{\alpha_t} x_{t-1} + \sqrt{1 - \alpha_t} z_{t-1} = \dots = \sqrt{\alpha_t} x_0 + \sqrt{1 - \alpha_t} z, \quad (5)$$

where  $x_t$  denotes the intermediate latent map at time step  $t$ ,  $z$  denotes the added noise,  $\beta_t$  denotes the standard deviation, and  $\alpha_t = 1 - \beta_t$  denotes the noise intensity. The standard deviation  $\beta_t$  of the noise added at each time step is specified and increases as  $t$  increases. The mean value of the noise added at each time step is adjusted according to  $\beta_t$ , in order to make sure that  $x_T$  converges stably to  $\mathcal{N}(0, 1)$ .

The Fourier transform is a classic transformation widely used in digital image processing. It transforms a time-domain signal into a

**Table 1: CLIP-based evaluations. The best results are in bold, and the second best results are underlined.**

Metric	Text Similarity↑				Image Similarity↑				
	Method	Reference	ProSpect	DreamBooth	TI	Reference	ProSpect	DreamBooth	TI
Average		0.2479	<b>0.3444</b>	<u>0.3334</u>	0.3115	0.9128	0.7927	<b>0.7987</b>	0.7274
Min		0.2168	<b>0.2869</b>	0.2279	<u>0.2371</u>	0.8771	<b>0.6899</b>	<u>0.6450</u>	0.4471
Max		0.2767	<b>0.3995</b>	0.3666	<u>0.3820</u>	0.9541	<b>0.929</b>	<u>0.8678</u>	0.8688
Negative Error		0.0311	0.0575	0.1055	0.0743	0.0357	0.1027	0.1537	0.2803
Positive Error		0.0288	0.0551	0.0331	0.0705	0.0412	0.1363	0.0691	0.1414

frequency-domain signal, facilitating the identification and processing of subtle features and challenging areas in the frequency domain. Grayscale images consist of discrete points in two dimensions, and the Two-Dimensional Discrete Fourier Transform (2D-DFT) is commonly used in image processing to obtain the frequency spectrum of an image that reflects its degree of grayscale variation. The center of the Fourier spectrum represents the low-frequency signal, whereas higher frequencies are represented by points closer to the edge. High-frequency signals typically correspond to edges and noise in the image, while the smooth areas of the image correspond to low-frequency signals. The Discrete Fourier Transform (DFT) of an image is formulated as:

$$F(u, v) = \sum_{x=0}^{M-1} \sum_{y=0}^{N-1} f(x, y) e^{-j2\pi(ux/M+vy/N)}, \quad (6)$$

where  $M$  and  $N$  denote the length and height of the image, respectively.  $F(u, v)$  denotes the frequency domain image, and  $f(x, y)$  represents the time domain image. The range of  $u$  is  $[0, M - 1]$ , and the range of  $v$  is  $[0, N - 1]$ .

Fig. 7 shows the Fourier spectrum of the diffusion process. As the number of steps in the denoising process increases, the high-frequency information contained in the image predicted by the diffusion model gradually increases. This indicates that the model tends to generate structural information at the start of the denoising process, with details gradually increasing as the steps increase. This phenomenon explains the generation order of the diffusion model, which is caused by the signal frequency of the corresponding attribute from low to high.

## 5 EXPERIMENTS

We demonstrate that *ProSpect* outperforms state-of-the-art text-to-image personalization baselines. We conduct both qualitative and quantitative evaluations, and our method achieves superior results in terms of both fidelity and editability. Moreover, we apply *ProSpect* to other applications of material transfer, style transfer, and layout transfer (as shown in Sec. 5.4), and perform qualitative comparisons with related methods.

*Compared Methods.* (1) **Textual Inversion (TI)** [28]: a SOTA method that learns a pseudo-word for a concept within a limited number of images using an optimization-based approach. (2) **DreamBooth** [87]: a SOTA method that learns a unique identifier and fine-tunes the diffusion model to learn the concept from a set of images. (3) **Perfusion** [94] is a recently released method that

obtains the concept by learning unique token embedding, and a dynamic key-locked rank-1 updating to the diffusion model, requiring fewer parameters to be fine-tuned. (4) **XTI** [97]: a recently released method that learns a more accurate and flexible concept by layer-wise prompt learning in the denoising U-Net inside the diffusion model. (5) **InstructPix2Pix** [11]: a SOTA image editing method that trains the diffusion model on their labeled training set and generates images with user-written instructions. (6) **InST** [108]: a SoTA diffusion-based style transfer method that obtains a representation of the overall appearance of the image by inverting the artistic image into a text condition.

*Implementation Details.* In all our experiments, we utilized Stable Diffusion 1.4 [85] with default hyperparameters and set a base learning rate of 0.001. We employed a DDIM sampler with diffusion steps  $T = 50$  and guidance scale  $w = 7.5$ . We used a frozen CLIP model in Stable Diffusion as the text encoder network. The texts were tokenized into start-token, end-token, and 75 non-text padding tokens. The training process on each image takes approximately 20 minutes using an NVIDIA GeForce RTX3090 with a batch size of 1, significantly less than the more than 90 minutes required for TI. The synthesis process takes about three seconds, depending on the number of diffusion steps taken.

### 5.1 Quantitative Evaluation

The following evaluation metrics are calculated: (1) The pair-wise CLIP cosine similarity between the reference images and the generated images. Image similarity is calculated to evaluate content fidelity. (2) The CLIP similarity between all generated images and their textual conditions. Text similarity is calculated to evaluate the editability.

Table 1 shows the quantitative evaluation results of our method and two baseline methods. The Reference column of text similarity calculates the cosine similarity between the reference image and the various text condition, which can be regarded as the lower bound score. The Reference column of image similarity calculates the cosine similarity between the image contains the same object and the reference image, which can be regarded as the groundtruth score. TI [28] fails to preserve object appearance, while DreamBooth tends to overfit the reference image. Though a higher fidelity score it gets, the editability is not satisfactory. Our method achieves a better balance of object fidelity and editability without fine-tuning the model.

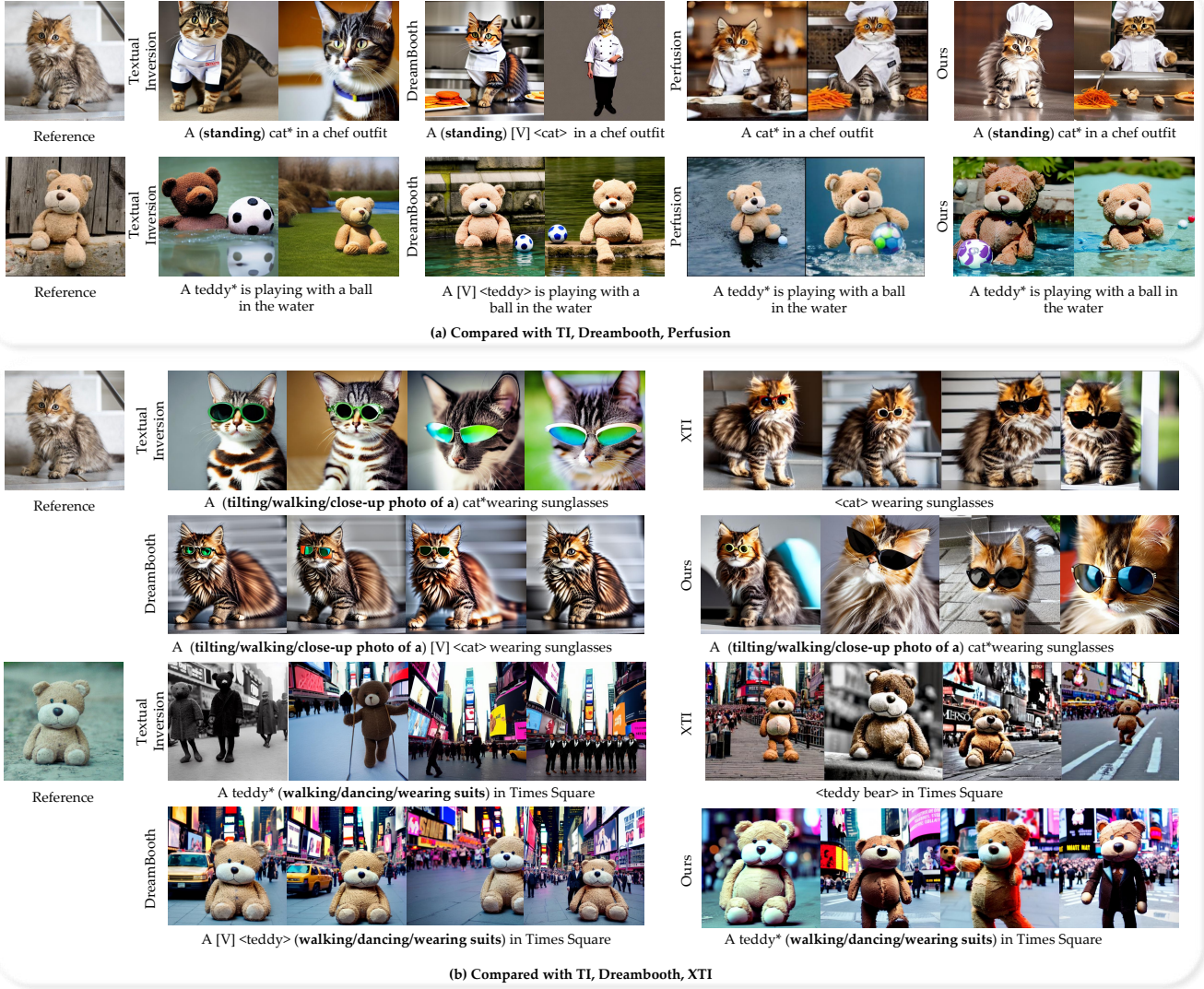


**Figure 8: Comparisons with state-of-the-art personalization methods including Textual Inversion (TI) [28], DreamBooth [87], XTI [97], and Perfusion [94].** The bold words correspond to the additional concepts added to each image, (e.g. the 3<sup>rd</sup> column in (a) shows the result of “*A standing cat in a chef outfit*”, the 6<sup>th</sup> column in (b) shows the result of “*A tilting cat wearing sunglasses*”). XTI and Perfusion are the latest published methods and the model have not been released yet. The resulting images of XTI and Perfusion are borrowed from their paper, so the results of adding concepts are not shown. Our method is faithful to convey the appearance and material of the reference image while having better controllability and diversity.

## 5.2 Qualitative Evaluation

As shown in Fig. 8, we compare our method with four SOTA personalization methods TI [28], DreamBooth [87], XTI [97] and Perfusion [94]. We use concepts from previous papers for fair and unbiased evaluation. As the codes of XTI and Perfusion have not been released yet, we borrow the result images shown in their papers for comparison purposes.

We add additional texts shown in **bold**, to each set of images to demonstrate the flexibility of our method. DreamBooth can well depict the conceptual appearance in the reference image, but tends

to overfit to the reference image, resulting in a lack of editability. As shown in the results of “*A (standing) cat in a chef outfit*” in the second row, TI fails to maintain the object’s appearance and generates normal cats. DreamBooth can generate a standing cat, but the background is blurred, and the cat’s paw is confused with the human hand. Our results can generate a standing cat with a kitchen as the background and maintain the details of the cat’s paws. The results of “*a (tilting/walking/close-up photo of a) cat wearing sunglasses*” show that DreamBooth can generate a cat with sunglasses, but cannot change the cat’s posture or zoom-in/zoom-out. Our method, shown in the third row, can generate high-fidelity concepts while



**Figure 9: Comparision with DreamBooth [87] method on one-shot portrait generation personalization. By applying our method to the inversion of characters, we can maintain the identity of the input image.**

maintaining diversity and flexibility. *ProSpect* not only puts sunglasses on the cat but also allows it to show its walking posture and close-up details. In the results “*A teddy is playing with a ball in the water*”, *Perfusion* and *DreamBooth* can generate teddy bear, ball, and water, but they are not interacting with each other. Our method can show the posture of the teddy bear touching and throwing the ball, and the teddy bear can float on the water or half-submerge in the water. In the results of “*A teddy (walking/dancing/wearing suits) in Times Square*”, *XTI* cannot accurately maintain the appearance of the teddy bear, and *DreamBooth* cannot change the posture of the teddy bear. Our method can reproduce the appearance of a teddy bear while walking, dancing, and wearing a suit, always in the background of Times Square.

Our method is also capable of one-shot portrait generation personalization. Fig. 9 displays the comparison results between our method and *DreamBooth* [87]. Our method can make changes to character clothing, hairstyles, artistic styles, etc. while maintaining identity.

### 5.3 User Study

We evaluate our method in attributes-aware image generation, alongside three SOTA personalization methods: *TI* [28], *DreamBooth* [87], and *InST* [108]. A total of 66 participants took part in the survey, including 42 researchers in computer graphics or computer vision, 24 university students. The user study was divided

into three parts: personalized objects, material guidance, and style guidance.

*User Study I.* In the content-aware image generation survey, *TI* and *DreamBooth* were used as the baseline methods. The objective of the personalization task, which was to generate a new image with the same concept as the reference image while also matching the provided text condition, was introduced to the participants. For each question, the participants were shown a reference image and a text condition (e.g., “*a photo of the same cat wearing sunglasses*”) and asked to choose the option that best matched the task objective from three randomly ordered options, each corresponding to a method. *ProSpect* received 51.97% of the preferences, while *TI* acquired 10.30%, and *DreamBooth* obtained 37.72%. Thus, *ProSpect* exhibited better performance in human preference when compared to the two baseline methods.

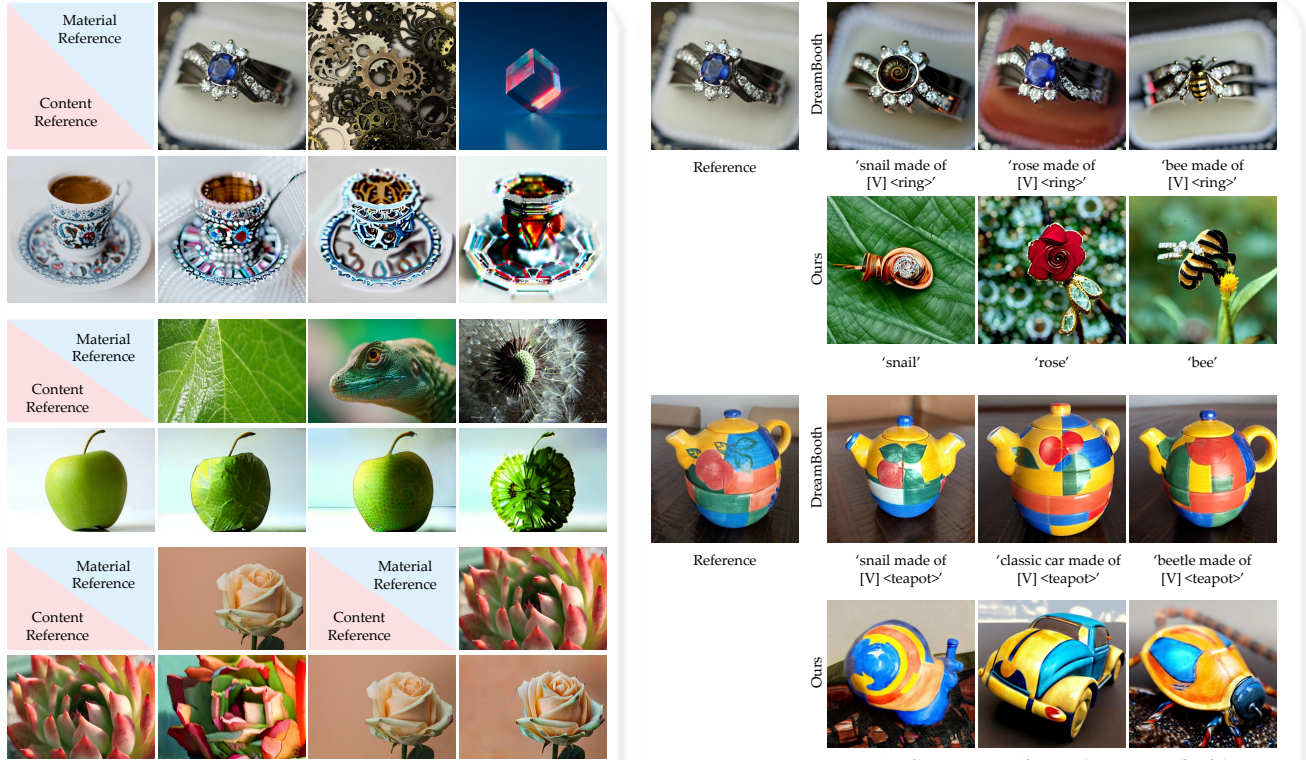
*User Study II.* In the material-aware image generation survey, *DreamBooth* was used as the baseline method, and the participants were introduced that the objective of the task was to generate a new image composed of materials from the reference image while matching the provided text conditions. For each question, the participants were shown reference images and corresponding text conditions (e.g., “*a snail made of the material in this image*”) and asked to select one of two options that best match the task objective. *ProSpect* received 66.36%’s preference and *DreamBooth* obtained 33.64%.

*User Study III.* The SOTA style transfer method *InST* [108] is the baseline method in style-aware image generation survey. We evaluate both the style-guided text-to-image generation task and the style transfer task. The participants were introduced that the objective of the task was to generate a new image consistent with the style of the reference artistic image while also being consistent with the content of the provided textual condition/content image. For each question, the participants were presented with either a style image and a corresponding text condition (e.g., “*a painting of Einstein drawn in the style of the reference image*”) or a pair of style and content images, and asked to select one of two options that best matched the task objective. *ProSpect* outperformed *InST* by receiving 61.67% the preference of compared with *InST*’s 38.33%.

### 5.4 Applications

In this section, we demonstrate the effectiveness of our approach in various attribute-aware image generation tasks, including material-aware image generation, style-aware image generation, as well as layout-aware image generation.

*Material-Aware Image Generation.* Our approach is well-suited for material-aware image generation tasks, including material transfer between images, image material-guided text-to-image generation, and image material editing with text. Results shown in Fig. 10 demonstrate the high visual quality and flexibility of our method. Fig. 10(a) shows the results of material transfer, where our method can transfer materials between semantically unrelated objects (e.g., gears and teacups, apples, and dandelions). Fig. 10(b) shows the material-guided text-to-image generation using a reference image, which we compare with a state-of-the-art personalization method



**(c) Real Image Material Editing via Text**

**Figure 10: Material-aware image generation results.** We compare *ProSpect* with a personalization approach *DreamBooth* [87] and an image editing approach *InstructPix2Pix* [11]. Our method shows better fidelity and editability.

*DreamBooth* [87]. *DreamBooth* requires both prompt learning and model fine-tuning, making it prone to overfitting on specific images and lacking flexibility with single-image input. Our method, however, can guide image generation using references with unrelated materials (e.g., rings and snails, teapot, and beetle), demonstrating superior editability. Fig. 10(c) shows the results of modifying an image’s material with natural language. We compare our method with a state-of-the-art image editing method *InstructPix2Pix* [11], which works on semantically related images (e.g., hummingbird to

peacock feather) but fails on semantically unrelated modifications (e.g., teddy to origami). Unlike *InstructPix2Pix*, our method can edit images into completely unrelated materials while retaining their overall appearance and background.

*Style-Aware Image Generation.* Our method is also effective for generating artistic images. The material in a realistic image reflects high-frequency information, while strokes and shapes reflect the same in an artistic image. Using a similar approach to material transfer, we can perform style transfer and style-guided text-to-image

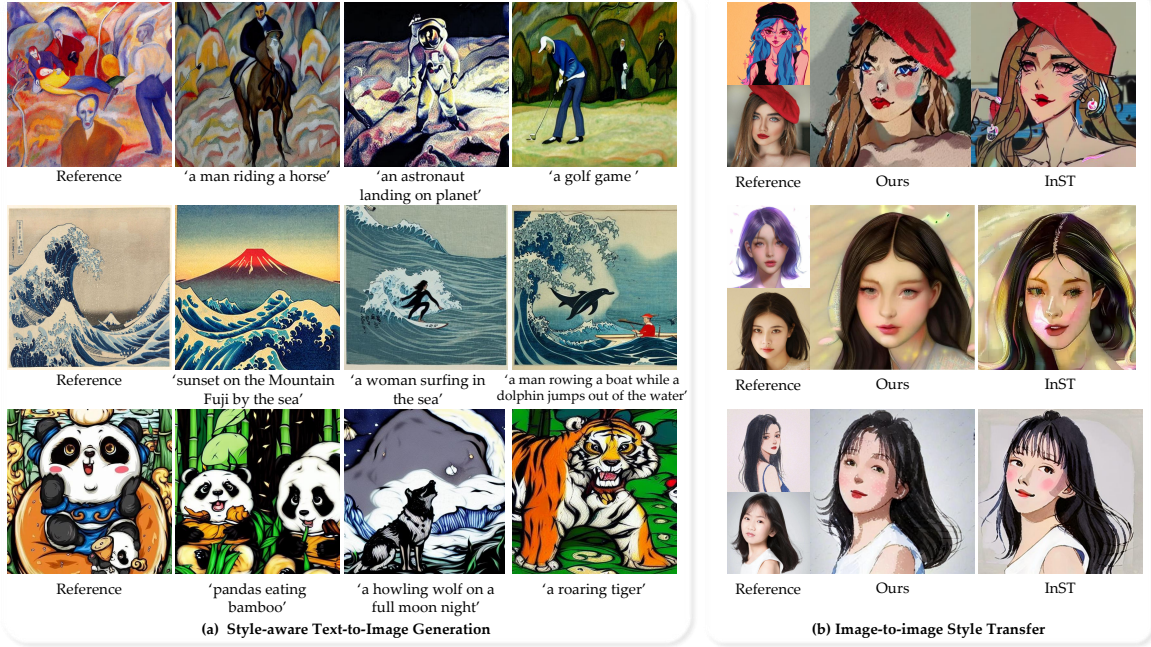


**Figure 11: Style-aware image generation results.** We compare *ProSpect* with a state-of-the-art diffusion-based style transfer method InST [108]. Our method better preserves the identity information of the content image and generate better brush strokes.

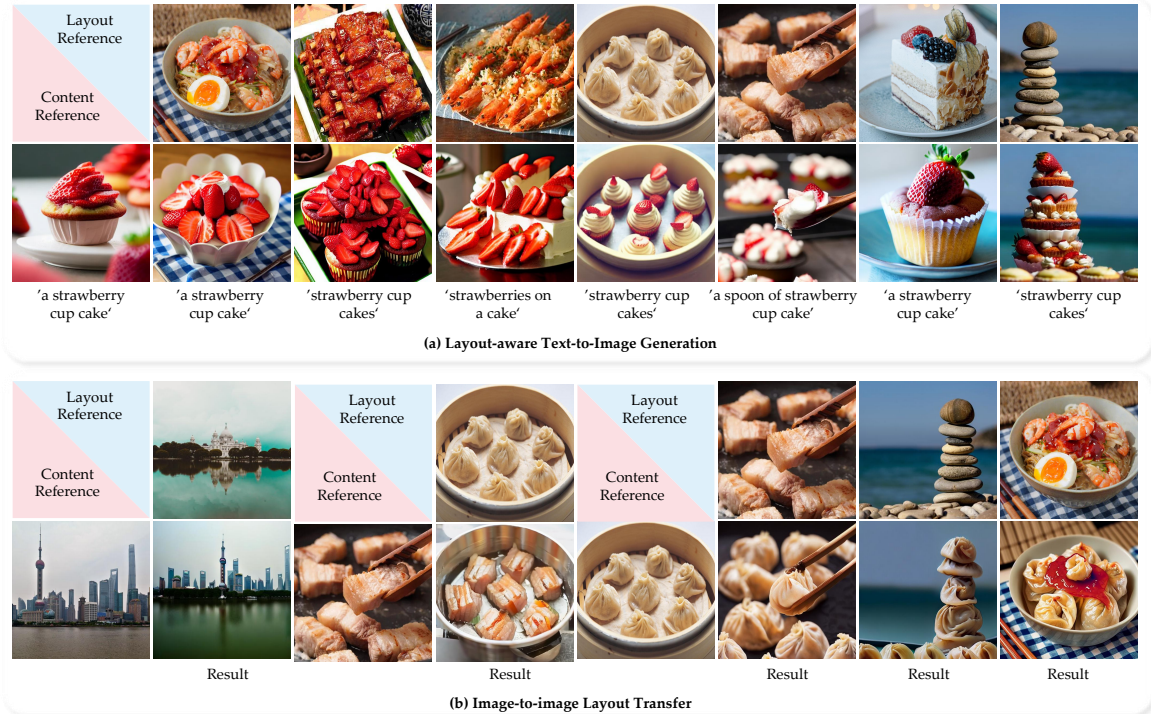


**Figure 12: Layout-aware image generation results.** *ProSpect* can generate an image with the same layout of an layout reference image by using a text prompt or a content reference image.



**Figure 13: Results of multiple attribute-aware image generation with *ProSpect*.** (a) Each reference offers one kind of visual attribute, and we combine them progressively to generate joint results by mixing the triplet references. (b) Each reference indicates two kinds of visual attributes, and we mix two references by taking the material/layout/style attribute from individual references and scaling the range of content conditions.

generation. Fig. 11(a) shows the results of style-guided text-to-image generation, where our method learns the style from a single artistic image and generates new images that are semantically different (e.g., “*an astronaut landing on a planet*”) or more vivid in content (e.g., “*a man rowing a boat while a dolphin jumps out of the water*”), while accurately reproducing the reference image’s style. Fig. 11(b) shows the results of style transfer, comparing it with the state-of-the-art diffusion-based style transfer method InST [108]. Since InST considers the overall appearance of an image as a condition and lacks disentanglement of style and content, the generated image often lacks identity. Our method produces more realistic strokes (e.g., the hair in 1<sup>st</sup> and 3<sup>rd</sup> rows), fewer artifacts (e.g. the 2<sup>nd</sup> row), and better-maintained identity.

**Layout-Aware Image Generation.** Layout is a core element of photography that determines the quality of a photo. The low-frequency information of an image reflects its layout. By learning this information, our method can use the layout of a single given image to guide text-to-image generation and transfer the layout of an image to another image. Fig. 12(a) shows the results of layout-guided text-to-image generation, where our method learns complex composition (e.g., “*a spoon of strawberry cupcake*”) and guides the generation of semantically unrelated content (e.g., strawberry cupcake and rock) from a reference image. Fig. 12(b) displays the results of layout transfer for landscape and still-life images. Our method can transfer the “centering” and “reflection” features of a photo to another landscape image (see the second column in Fig. 12(b)) and transfer complex object layouts to another still-life image.

**Multiple Attribute-Aware Image Generation.** In Fig. 13, we combine attributes from multiple images to guide the generation process.

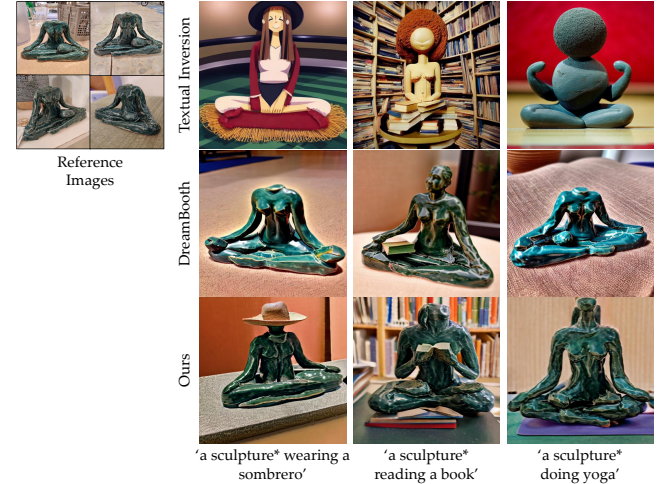


**Figure 14: Our results by training with a small number of images.**

In Fig. 13(a), the layout, content, and style are guided by three reference images. Results for a landscape example are shown in the left pink pyramid. The first row displays reference images, the second row displays results using dual-attribute guidance, and the bottom row shows the result using triple-attribute guidance. The bottom result maintains the relative position of the flowers and architecture in the layout image, has the three-floor building structure from the content reference, and replicates the appearance of Chinese architecture from the style reference. In the right blue pyramid, we show results for a portrait example. The top result is guided by the layout of a single person in the middle, the content of a cyclist,

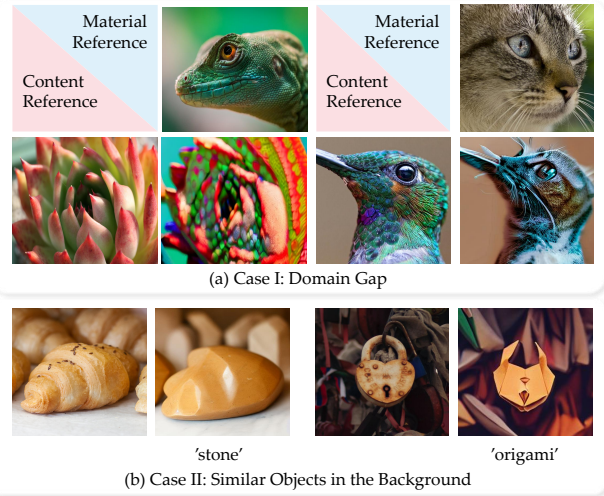


**Figure 15: Examples of limitations. (a) Results of transferring materials between images with large domain gaps. (b) When the image background is composed of similar objects sharing the same frequency information, attribute editing may be applied to the entire image.**

and the style of an astronaut. Fig. 13(b) shows a different setting by mixing multiple attributes from one image.

*More than One-Shot.* *ProSpect* is designed to accept a single image as input, but it can also work on a group of images, similar to TI [28] or DreamBooth [87]. As shown in Fig. 14, *ProSpect* can produce results with improved fidelity and diversity compared to prior approaches when applied to four sculpture images. In addition, *ProSpect* can also be applied to model fine-tuning methods.

## 5.5 Limitations

Firstly, although *ProSpect* is faster than TI, it is still not as fast as some encoder-based methods [29], given that each iteration of optimizations is calculated on a random step and *ProSpect* learns several token embeddings at different steps. Secondly, as shown in Fig. 15(a), though *ProSpect* can achieve attribute disentanglement, attribute transfer between images with large domain gap is not always visually aesthetic. Finally, Fig. 15(b) shows the results of the cases when dealing with images whose background is composed of similar objects. Since the same attribute of the same object is in the same scale, sometimes the attribute modification may act on the background objects, too.

## 6 CONCLUSION AND FUTURE WORK

In this paper, we delve into the image generation process of the diffusion model from the perspective of steps. We propose an expanded textual conditioning space, denoted by  $\mathcal{P}^*$ , which is based on CLIP and diffusion models. Our experiments demonstrate that  $\mathcal{P}^*$  has better disentanglement and controllability, allowing for generating images from different granularities. To further enable images to be represented in  $\mathcal{P}^*$ , we propose *ProSpect*, which inverts the diffusion model step-by-step. *ProSpect* provides more fidelity and editable

image representations, paving the way for attributes-aware image generation. Using *ProSpect*, material/style/content/layout-related transfer and editing tasks can be performed. Our evaluations and experimental results demonstrate that *ProSpect* offers a superior fidelity, expressiveness, and controllable approach to developing diverse image generation tasks. In the future work, we plan to further analyze the method of attribute disentanglement, such as making a more detailed attribute division and recombination methods and studying the mutual influence of different textual conditions.

## REFERENCES

- [1] 1984. *SIGCOMM Comput. Commun. Rev.* 13–14, 5–1 (1984).
- [2] 2008. *CHI '08: CHI '08 extended abstracts on Human factors in computing systems* (Florence, Italy). ACM, New York, NY, USA. General Chair-Czerwinski, Mary and General Chair-Lund, Arnie and Program Chair-Tan, Desney.
- [3] Rafal Ablamowicz and Bertfried Fauser. 2007. *CLIFFORD: a Maple 11 Package for Clifford Algebra Computations, version 11.* Retrieved February 28, 2008 from <http://math.tntech.edu/rafal/cliff11/index.html>
- [4] Patricia S. Abril and Robert Plant. 2007. The patent holder’s dilemma: Buy, sell, or troll? *Commun. ACM* 50, 1 (Jan. 2007), 36–44. <https://doi.org/10.1145/1188913.1188915>
- [5] Sten Andler. 1979. Predicate Path expressions. In *Proceedings of the 6th ACM SIGACT-SIGPLAN symposium on Principles of Programming Languages (POPL '79)*. ACM Press, New York, NY, 226–236. <https://doi.org/10.1145/567752.567774>
- [6] David A. Anisi. 2003. *Optimal Motion Control of a Ground Vehicle*. Master’s thesis. Royal Institute of Technology (KTH), Stockholm, Sweden.
- [7] Omri Avrahami, Dani Lischinski, and Ohad Fried. 2022. Blended Diffusion for Text-Driven Editing of Natural Images. In *IEEE/CVF Conference on Computer Vision and Pattern Recognition (CVPR)*. 18208–18218.
- [8] Yogesh Balaji, Seungjun Nah, Xun Huang, Arash Vahdat, Jiaming Song, Karsten Kreis, Miika Aittala, Timo Aila, Samuli Laine, Bryan Catanzaro, et al. 2022. ediffi: Text-to-image diffusion models with an ensemble of expert denoisers. *arXiv preprint arXiv:2211.01324* (2022).
- [9] David Bau, Alex Andonian, Audrey Cui, YeonHwan Park, Ali Jahanian, Aude Oliva, and Antonio Torralba. 2021. Paint by word. *arXiv preprint arXiv:2103.10951* (2021).
- [10] Andrew Brock, Jeff Donahue, and Karen Simonyan. 2019. Large Scale GAN Training for High Fidelity Natural Image Synthesis. *International Conference on Learning Representations (ICLR)* (2019).
- [11] Tim Brooks, Aleksander Holynski, and Alexei A Efros. 2023. InstructPix2Pix: Learning to Follow Image Editing Instructions. In *IEEE/CVF Conference on Computer Vision and Pattern Recognition (CVPR)*. 18392–18402.
- [12] Jonathan F. Buss, Arnold L. Rosenberg, and Judson D. Knott. 1987. *Vertex Types in Book-Embeddings*. Technical Report. Amherst, MA, USA.
- [13] Jonathan F. Buss, Arnold L. Rosenberg, and Judson D. Knott. 1987. *Vertex Types in Book-Embeddings*. Technical Report. Amherst, MA, USA.
- [14] Huiwen Chang, Han Zhang, Jarred Barber, AJ Maschinot, Jose Lezama, Lu Jiang, Ming-Hsuan Yang, Kevin Murphy, William T Freeman, Michael Rubinstein, et al. 2023. Muse: Text-To-Image Generation via Masked Generative Transformers. *arXiv preprint arXiv:2301.00704* (2023).
- [15] Kenneth L. Clarkson. 1985. *Algorithms for Closest-Point Problems (Computational Geometry)*. Ph. D. Dissertation. Stanford University, Palo Alto, CA. UMI Order Number: AAT 8506171.
- [16] Kenneth Lee Clarkson. 1985. *Algorithms for Closest-Point Problems (Computational Geometry)*. Ph. D. Dissertation. Stanford University, Stanford, CA, USA. Advisor(s) Yao, Andrew C. AAT 8506171.
- [17] Jacques Cohen (Ed.). 1996. Special issue: Digital Libraries. *Commun. ACM* 39, 11 (Nov. 1996).
- [18] Sarah Cohen, Werner Nutt, and Yehoshua Sagiv. 2007. Deciding equivalences among conjunctive aggregate queries. *J. ACM* 54, 2, Article 5 (April 2007), 50 pages. <https://doi.org/10.1145/1219092.1219093>
- [19] Mauro Conti, Roberto Di Pietro, Luigi V. Mancini, and Alessandro Mei. 2009. (new) Distributed data source verification in wireless sensor networks. *Inf. Fusion* 10, 4 (Oct. 2009), 342–353. <https://doi.org/10.1016/j.inffus.2009.01.002>
- [20] Mauro Conti, Roberto Di Pietro, Luigi V. Mancini, and Alessandro Mei. 2009. (old) Distributed data source verification in wireless sensor networks. *Inf. Fusion* 10, 4 (2009), 342–353. <https://doi.org/10.1016/j.inffus.2009.01.002>
- [21] Katherine Crowson, Stella Biderman, Daniel Kornis, Dashill Stander, Eric Hallahan, Louis Castricato, and Edward Raff. 2022. VQGAN-CLIP: Open domain image generation and editing with natural language guidance. In *European Conference on Computer Vision (ECCV)*. Springer, 88–105.
- [22] Prafulla Dhariwal and Alexander Nichol. 2021. Diffusion models beat GANs on image synthesis. In *Advances in Neural Information Processing Systems (NeurIPS)*. 8780–8794.

[23] Bruce P. Douglass, David Harel, and Mark B. Trakhtenbrot. 1998. Statecharts in use: structured analysis and object-orientation. In *Lectures on Embedded Systems*, Grzegorz Rozenberg and Frits W. Vaandrager (Eds.). Lecture Notes in Computer Science, Vol. 1494. Springer-Verlag, London, 368–394. [https://doi.org/10.1007/3-540-65193-4\\_29](https://doi.org/10.1007/3-540-65193-4_29)

[24] Ian Editor (Ed.). 2007. *The title of book one* (1st. ed.). The name of the series one, Vol. 9. University of Chicago Press, Chicago. <https://doi.org/10.1007/3-540-09237-4>

[25] Ian Editor (Ed.). 2008. *The title of book two* (2nd. ed.). University of Chicago Press, Chicago, Chapter 100. <https://doi.org/10.1007/3-540-09237-4>

[26] Patrick Esser, Robin Rombach, and Björn Ommer. 2021. Taming Transformers for High-Resolution Image Synthesis. In *IEEE/CVF Conference on Computer Vision and Pattern Recognition (CVPR)*. 12873–12883.

[27] Oran Gafni, Adam Polyak, Oron Ashual, Shelly Sheynin, Devi Parikh, and Yaniv Taigman. 2022. Make-a-scene: Scene-based text-to-image generation with human priors. In *European Conference on Computer Vision (ECCV)*. Springer, 89–106.

[28] Rinon Gal, Yuval Alaluf, Yuval Atzmon, Or Patashnik, Amit H Bermano, Gal Chechik, and Daniel Cohen-Or. 2023. An Image is Worth One Word: Personalizing Text-to-Image Generation using Textual Inversion. In *International Conference on Learning Representations (ICLR)*.

[29] Rinon Gal, Moab Arar, Yuval Atzmon, Amit H Bermano, Gal Chechik, and Daniel Cohen-Or. 2023. Encoder-based Domain Tuning for Fast Personalization of Text-to-Image Models. In *ACM SIGGRAPH*.

[30] Rinon Gal, Or Patashnik, Haggai Maron, Amit H. Bermano, Gal Chechik, and Daniel Cohen-Or. 2022. StyleGAN-NADA: CLIP-Guided Domain Adaptation of Image Generators. *ACM Transactions on Graphics* 41, 4, Article 141 (jul 2022), 13 pages.

[31] Dan Geiger and Christopher Meek. 2005. Structured Variational Inference Procedures and their Realizations (as incol). In *Proceedings of Tenth International Workshop on Artificial Intelligence and Statistics*, The Barbados. The Society for Artificial Intelligence and Statistics.

[32] Ian Goodfellow, Jean Pouget-Abadie, Mehdi Mirza, Bing Xu, David Warde-Farley, Sherjil Ozair, Aaron Courville, and Yoshua Bengio. 2014. Generative Adversarial Nets. In *Advances in Neural Information Processing Systems (NIPS)*. Curran Associates, Inc.

[33] Michel Goossens, S. P. Rahtz, Ross Moore, and Robert S. Sutor. 1999. *The Latex Web Companion: Integrating TEX, HTML, and XML* (1st ed.). Addison-Wesley Longman Publishing Co., Inc., Boston, MA, USA.

[34] Matthew Van Gundy, Davide Balzarotti, and Giovanni Vigna. 2007. Catch me, if you can: Evading network signatures with web-based polymorphic worms. In *Proceedings of the first USENIX workshop on Offensive Technologies (WOOT '07)*. USENIX Association, Berkley, CA, Article 7, 9 pages.

[35] Matthew Van Gundy, Davide Balzarotti, and Giovanni Vigna. 2008. Catch me, if you can: Evading network signatures with web-based polymorphic worms. In *Proceedings of the first USENIX workshop on Offensive Technologies (WOOT '08)*. USENIX Association, Berkley, CA, Article 7, 2 pages.

[36] Matthew Van Gundy, Davide Balzarotti, and Giovanni Vigna. 2009. Catch me, if you can: Evading network signatures with web-based polymorphic worms. In *Proceedings of the first USENIX workshop on Offensive Technologies (WOOT '09)*. USENIX Association, Berkley, CA, 90–100.

[37] David Harel. 1978. *LOGICS of Programs: AXIOMATICS and DESCRIPTIVE POWER*. MIT Research Lab Technical Report TR-200. Massachusetts Institute of Technology, Cambridge, MA.

[38] David Harel. 1979. *First-Order Dynamic Logic*. Lecture Notes in Computer Science, Vol. 68. Springer-Verlag, New York, NY. <https://doi.org/10.1007/3-540-09237-4>

[39] Amir Hertz, Ron Mokady, Jay Tenenbaum, Kfir Aberman, Yael Pritch, and Daniel Cohen-Or. 2023. Prompt-to-Prompt Image Editing with Cross Attention Control. In *International Conference on Learning Representations (ICLR)*.

[40] Aaron Hertzmann, Charles E Jacobs, Nuria Oliver, Brian Curless, and David H Salesin. 2001. Image analogies. In *Proceedings of the 28th annual conference on Computer graphics and interactive techniques*. 327–340.

[41] Martin Heusel, Hubert Ramsauer, Thomas Unterthiner, Bernhard Nessler, and Sepp Hochreiter. 2017. GANs Trained by a Two Time-Scale Update Rule Converge to a Local Nash Equilibrium. In *Advances in Neural Information Processing Systems (NIPS)*.

[42] Billy S. Hollis. 1999. *Visual Basic 6: Design, Specification, and Objects with Other* (1st ed.). Prentice Hall PTR, Upper Saddle River, NJ, USA.

[43] Lianghua Huang, Di Chen, Yu Liu, Yujun Shen, Deli Zhao, and Jingren Zhou. 2023. Composer: Creative and controllable image synthesis with composable conditions. *arXiv preprint arXiv:2302.09778* (2023).

[44] Lianghua Huang, Di Chen, Yu Liu, Shen Yujun, Deli Zhao, and Zhou Jingren. 2023. Composer: Creative and Controllable Image Synthesis with Composable Conditions. (2023).

[45] Nisha Huang, Fan Tang, Weiming Dong, Tong-Yee Lee, and Changsheng Xu. 2023. Region-Aware Diffusion for Zero-shot Text-driven Image Editing. *arXiv preprint arXiv:2302.11797* (2023).

[46] Nisha Huang, Fan Tang, Weiming Dong, and Changsheng Xu. 2022. Draw Your Art Dream: Diverse Digital Art Synthesis with Multimodal Guided Diffusion. In *ACM International Conference on Multimedia* (Lisboa, Portugal). 1085–1094.

[47] Nisha Huang, Yuxin Zhang, Fan Tang, Chongyang Ma, Haibin Huang, Yong Zhang, Weiming Dong, and Changsheng Xu. 2022. DiffStyler: Controllable Dual Diffusion for Text-Driven Image Stylization. *arXiv preprint arXiv:2211.10682* (2022).

[48] Ziqi Huang, Tianxing Wu, Yuming Jiang, Kelvin CK Chan, and Ziwei Liu. 2023. ReVersion: Diffusion-Based Relation Inversion from Images. *arXiv preprint arXiv:2303.13495* (2023).

[49] IEEE 2004. IEEE TCSC Executive Committee. In *Proceedings of the IEEE International Conference on Web Services (ICWS '04)*. IEEE Computer Society, Washington, DC, USA, 21–22. <https://doi.org/10.1109/ICWS.2004.64>

[50] Jaeseok Jeong, Mungi Kwon, and Youngjung Uh. 2023. Training-free Style Transfer Emerges from h-space in Diffusion models. *arXiv preprint arXiv:2303.15403* (2023).

[51] Bahjat Kawar, Shiran Zada, Oran Lang, Omer Tov, Huiwen Chang, Tali Dekel, Inbar Mosseri, and Michal Irani. 2023. Imagic: Text-Based Real Image Editing with Diffusion Models. In *IEEE/CVF Conference on Computer Vision and Pattern Recognition (CVPR)*. 6007–6017.

[52] Donald E. Knuth. 1981. *Seminarical Algorithms*. Addison-Wesley.

[53] Donald E. Knuth. 1997. *The Art of Computer Programming*, Vol. 1: *Fundamental Algorithms* (3rd. ed.). Addison Wesley Longman Publishing Co., Inc.

[54] Donald E. Knuth. 1998. *The Art of Computer Programming* (3rd ed.). Fundamental Algorithms, Vol. 1. Addison Wesley Longman Publishing Co., Inc. (book).

[55] Wei-Chang Kong. 2001. *E-commerce and cultural values*. IGI Publishing, Hershey, PA, USA, Name of chapter: The implementation of electronic commerce in SMEs in Singapore (Inbook-w-chap-w-type), 51–74. <http://portal.acm.org/citation.cfm?id=887006.887010>

[56] Wei-Chang Kong. 2001. The implementation of electronic commerce in SMEs in Singapore (as Incoll). In *E-commerce and cultural values*. IGI Publishing, Hershey, PA, USA, 51–74. <http://portal.acm.org/citation.cfm?id=887006.887010>

[57] Wei-Chang Kong. 2002. Chapter 9. In *E-commerce and cultural values (Incoll-w-text (chap 9) 'title')*, Theerasak Thanasanit (Ed.). IGI Publishing, Hershey, PA, USA, 51–74. <http://portal.acm.org/citation.cfm?id=887006.887010>

[58] Wei-Chang Kong. 2003. The implementation of electronic commerce in SMEs in Singapore (Incoll). In *E-commerce and cultural values*, Theerasak Thanasanit (Ed.). IGI Publishing, Hershey, PA, USA, 51–74. <http://portal.acm.org/citation.cfm?id=887006.887010>

[59] Wei-Chang Kong. 2004. *E-commerce and cultural values - (InBook-num-in-chap)*. IGI Publishing, Hershey, PA, USA, Chapter 9, 51–74. <http://portal.acm.org/citation.cfm?id=887006.887010>

[60] Wei-Chang Kong. 2005. *E-commerce and cultural values (Inbook-text-in-chap)*. IGI Publishing, Hershey, PA, USA, Chapter: The implementation of electronic commerce in SMEs in Singapore, 51–74. <http://portal.acm.org/citation.cfm?id=887006.887010>

[61] Wei-Chang Kong. 2006. *E-commerce and cultural values (Inbook-num chap)*. IGI Publishing, Hershey, PA, USA, Chapter (in type field) 22, 51–74. <http://portal.acm.org/citation.cfm?id=887006.887010>

[62] David Kosiur. 2001. *Understanding Policy-Based Networking* (2nd. ed.). Wiley, New York, NY.

[63] Nupur Kumari, Bingliang Zhang, Richard Zhang, Eli Shechtman, and Jun-Yan Zhu. 2023. Multi-Concept Customization of Text-to-Image Diffusion. In *IEEE/CVF Conference on Computer Vision and Pattern Recognition (CVPR)*. 1931–1941.

[64] Nupur Kumari, Bingliang Zhang, Richard Zhang, Eli Shechtman, and Jun-Yan Zhu. 2023. Multi-Concept Customization of Text-to-Image Diffusion. In *IEEE/CVF Conference on Computer Vision and Pattern Recognition (CVPR)*.

[65] Gihyun Kwon and Jong Chul Ye. 2022. CLIPstyler: Image Style Transfer with a Single Text Condition. In *IEEE/CVF Conference on Computer Vision and Pattern Recognition (CVPR)*. 18062–18071.

[66] Newton Lee. 2005. Interview with Bill Kinder: January 13, 2005. Video. *Comput. Entertain.* 3, 1, Article 4 (Jan.–March 2005). <https://doi.org/10.1145/1057270.1057278>

[67] Cheng-Lun Li, Ayse G. Buyuktur, David K. Hutchful, Natasha B. Sant, and Satyendra K. Narinwal. 2008. Portalis: using competitive online interactions to support aid initiatives for the homeless. In *CHI '08 extended abstracts on Human factors in computing systems* (Florence, Italy). ACM, New York, NY, USA, 3873–3878. <https://doi.org/10.1145/1358628.1358946>

[68] Senmao Li, Joost van de Weijer, Taihang Hu, Fahad Shahbaz Khan, Qibin Hou, Yaxing Wang, and Jian Yang. 2023. StyleDiffusion: Prompt-Embedding Inversion for Text-Based Editing. *arXiv preprint arXiv:2303.15649* (2023).

[69] Wentong Liao, Kai Hu, Michael Ying Yang, and Bodo Rosenhahn. 2022. Text to Image Generation with Semantic-Spatial Aware GAN. In *IEEE/CVF Conference on Computer Vision and Pattern Recognition (CVPR)*. 18187–18196.

[70] Andreas Lugmayr, Martin Danelljan, Andres Romero, Fisher Yu, Radu Timofte, and Luc Van Gool. 2022. RePaint: Inpainting Using Denoising Diffusion Probabilistic Models. In *IEEE/CVF Conference on Computer Vision and Pattern Recognition (CVPR)*. 18187–18196.

*Recognition (CVPR)*. 11461–11471.

[71] Kevin Meng, David Bau, Alex Andonian, and Yonatan Belinkov. 2022. Locating and editing factual associations in GPT. In *Advances in Neural Information Processing Systems (NeurIPS)*. 17359–17372.

[72] Ron Mokady, Amir Hertz, Kfir Aberman, Yael Pritch, and Daniel Cohen-Or. 2023. Null-text Inversion for Editing Real Images using Guided Diffusion Models. In *IEEE/CVF Conference on Computer Vision and Pattern Recognition (CVPR)*. 6038–6047.

[73] Sape Mullender (Ed.). 1993. *Distributed systems (2nd Ed.)*. ACM Press/Addison-Wesley Publishing Co., New York, NY, USA.

[74] Alex Nichol, Prafulla Dhariwal, Aditya Ramesh, Pranav Shyam, Pamela Mishkin, Bob McGrew, Ilya Sutskever, and Mark Chen. 2022. GLIDE: Towards photo-realistic image generation and editing with text-guided diffusion models. In *International Conference on Machine Learning (ICML)*.

[75] Alexander Quinn Nichol and Prafulla Dhariwal. 2021. Improved denoising diffusion probabilistic models. In *International Conference on Machine Learning (ICML)*. 8162–8171.

[76] Dave Novak. 2003. Solder man. Video. In *ACM SIGGRAPH 2003 Video Review on Animation theater Program: Part I - Vol. 145 (July 27–27, 2003)*. ACM Press, New York, NY, 4. <https://doi.org/10.1145/99.9999/woot07-S422>

[77] Barack Obama. 2008. A more perfect union. Video. Retrieved March 21, 2008 from <http://video.google.com/videoplay?docid=6528042696351994555>

[78] Or Patashnik, Zongze Wu, Eli Shechtman, Daniel Cohen-Or, and Dani Lischinski. 2021. StyleCLIP: Text-Driven Manipulation of StyleGAN Imagery. In *IEEE/CVF International Conference on Computer Vision (ICCV)*. 2085–2094.

[79] Charles J. Petrie. 1986. *New Algorithms for Dependency-Directed Backtracking* (Master’s thesis). Technical Report. Austin, TX, USA.

[80] Charles J. Petrie. 1986. *New Algorithms for Dependency-Directed Backtracking* (Master’s thesis). Master’s thesis. University of Texas at Austin, Austin, TX, USA.

[81] Poker-Edge.Com. 2006. Stats and Analysis. Retrieved June 7, 2006 from <http://www.poker-edge.com/stats.php>

[82] Alec Radford, Jong Wook Kim, Chris Hallacy, Aditya Ramesh, Gabriel Goh, Sandhini Agarwal, Girish Sastry, Amanda Askell, Pamela Mishkin, Jack Clark, et al. 2021. Learning transferable visual models from natural language supervision. In *International Conference on Machine Learning (ICML)*. 8748–8763.

[83] Aditya Ramesh, Prafulla Dhariwal, Alex Nichol, Casey Chu, and Mark Chen. 2022. Hierarchical Text-Conditional Image Generation with CLIP Latents. *arXiv preprint arXiv:2204.06125* (2022).

[84] Aditya Ramesh, Mikhail Pavlov, Gabriel Goh, Scott Gray, Chelsea Voss, Alec Radford, Mark Chen, and Ilya Sutskever. 2021. Zero-shot text-to-image generation. In *International Conference on Machine Learning (ICML)*. PMLR, 8821–8831.

[85] Robin Rombach, Andreas Blattmann, Dominik Lorenz, Patrick Esser, and Björn Ommer. 2022. High-resolution image synthesis with latent diffusion models. In *IEEE/CVF Conference on Computer Vision and Pattern Recognition (CVPR)*. 10684–10695.

[86] Bernard Rous. 2008. The Enabling of Digital Libraries. *Digital Libraries* 12, 3, Article 5 (July 2008). To appear.

[87] Nataniel Ruiz, Yuanzhen Li, Varun Jampani, Yael Pritch, Michael Rubinstein, and Kfir Aberman. 2023. DreamBooth: Fine tuning text-to-image diffusion models for subject-driven generation. In *IEEE/CVF Conference on Computer Vision and Pattern Recognition (CVPR)*. 22500–22510.

[88] Chitwan Saharia, William Chan, Saurabh Saxena, Lala Li, Jay Whang, Emily L Denton, Kamyar Ghasemipour, Raphael Gontijo Lopes, Burcu Karagol Ayan, Tim Salimans, et al. 2022. Photorealistic text-to-image diffusion models with deep language understanding. In *Advances in Neural Information Processing Systems (NeurIPS)*. 36479–36494.

[89] Peter Schaldenbrand, Zhixuan Liu, and Jean Oh. 2022. StyleCLIPDraw: Coupling Content and Style in Text-to-Drawing Translation. In *International Joint Conference on Artificial Intelligence (IJCAI)*. International Joint Conferences on Artificial Intelligence Organization, 4966–4972.

[90] Joseph Scientist. 2009. The fountain of youth. Patent No. 12345, Filed July 1st, 2008, Issued Aug. 9th, 2009.

[91] Stan W. Smith. 2010. An experiment in bibliographic mark-up: Parsing metadata for XML export. In *Proceedings of the 3rd. annual workshop on Librarians and Computers (LAC '10, Vol. 3)*. Reginald N. Smythe and Alexander Noble (Eds.). Paparazzi Press, Milan Italy, 422–431. <https://doi.org/10.1145/99.9999/woot07-S422>

[92] Asad Z. Spector. 1990. Achieving application requirements. In *Distributed Systems* (2nd. ed.), Sape Mullender (Ed.). ACM Press, New York, NY, 19–33. <https://doi.org/10.1145/90417.90738>

[93] Ming Tao, Hao Tang, Fei Wu, Xiaoyuan Jing, Bing-Kun Bao, and Changsheng Xu. 2022. DF-GAN: A Simple and Effective Baseline for Text-to-Image Synthesis. In *IEEE/CVF Conference on Computer Vision and Pattern Recognition (CVPR)*. 16494–16504.

[94] Yoad Tewel, Rinon Gal, Gal Chechik, and Yuval Atzmon. 2023. Key-Locked Rank One Editing for Text-to-Image Personalization. *ACM Transactions on Graphics* 42, 4 (jul 2023), 15 pages.

[95] Harry Thurnburg. 2001. *Introduction to Bayesian Statistics*. Retrieved March 2, 2005 from <http://ccrma.stanford.edu/~jos/bayes/bayes.html>

[96] Dani Valevski, Matan Kalman, Yossi Matias, and Yaniv Leviathan. 2022. UniTune: Text-driven image editing by fine tuning an image generation model on a single image. *arXiv preprint arXiv:2210.09477* (2022).

[97] Andrey Voynov, Qinghao Chu, Daniel Cohen-Or, and Kfir Aberman. 2023. P+: Extended Textual Conditioning in Text-to-Image Generation. *arXiv preprint arXiv:2303.09522* (2023).

[98] Yuxin Wen, Neel Jain, John Kirchenbauer, Micah Goldblum, Jonas Geiping, and Tom Goldstein. 2023. Hard prompts made easy: Gradient-based discrete optimization for prompt tuning and discovery. *arXiv preprint arXiv:2302.03668* (2023).

[99] Renato Werneck, João Setubal, and Arlindo da Conceição. 2000. (new) Finding minimum congestion spanning trees. *J. Exp. Algorithms* 5, Article 11 (Dec. 2000). <https://doi.org/10.1145/351827.384253>

[100] Renato Werneck, João Setubal, and Arlindo da Conceição. 2000. (old) Finding minimum congestion spanning trees. *J. Exp. Algorithms* 5 (2000), 11. <https://doi.org/10.1145/351827.384253>

[101] Qiucheng Wu, Yujian Liu, Handong Zhao, Ajinkya Kale, Trung Bui, Tong Yu, Zhe Lin, Yang Zhang, and Shiyu Chang. 2023. Uncovering the Disentanglement Capability in Text-to-Image Diffusion Models. In *IEEE/CVF Conference on Computer Vision and Pattern Recognition (CVPR)*. 1900–1910.

[102] Tao Xu, Pengchuan Zhang, Qiuyuan Huang, Han Zhang, Zhe Gan, Xiaolei Huang, and Xiaodong He. 2018. AttnGAN: Fine-Grained Text to Image Generation with Attentional Generative Adversarial Networks. In *IEEE/CVF Conference on Computer Vision and Pattern Recognition (CVPR)*. 1316–1324.

[103] Binxin Yang, Shuyang Gu, Bo Zhang, Ting Zhang, Xuejin Chen, Xiaoyan Sun, Dong Chen, and Fang Wen. 2023. Paint by Example: Exemplar-based Image Editing with Diffusion Models. In *IEEE/CVF Conference on Computer Vision and Pattern Recognition (CVPR)*. 18381–18391.

[104] Serin Yang, Hyunmin Hwang, and Jong Chul Ye. 2023. Zero-Shot Contrastive Loss for Text-Guided Diffusion Image Style Transfer. *arXiv preprint arXiv:2303.08622* (2023).

[105] Hui Ye, Xiulong Yang, Martin Takac, Rajshekhar Sunderraman, and Shihao Ji. 2021. Improving text-to-image synthesis using contrastive learning. *arXiv preprint arXiv:2107.02423* (2021).

[106] Jiahui Yu, Yuanzhong Xu, Jing Yu Koh, Thang Luong, Gunjan Baid, Zirui Wang, Vijay Vasudevan, Alexander Ku, Yinfei Yang, Burcu Karagol Ayan, et al. 2022. Scaling autoregressive models for content-rich text-to-image generation. *arXiv preprint arXiv:2206.10789* (2022).

[107] Han Zhang, Jing Yu Koh, Jason Baldridge, Honglak Lee, and Yinfei Yang. 2021. Cross-Modal Contrastive Learning for Text-to-Image Generation. In *IEEE/CVF Conference on Computer Vision and Pattern Recognition (CVPR)*. 833–842.

[108] Yuxin Zhang, Nisha Huang, Fan Tang, Haibin Huang, Chongyang Ma, Weiming Dong, and Changsheng Xu. 2023. Inversion-Based Style Transfer with Diffusion Models. In *IEEE/CVF Conference on Computer Vision and Pattern Recognition (CVPR)*. 10146–10156.

[109] Zhixing Zhang, Ligong Han, Arnab Ghosh, Dimitris Metaxas, and Jian Ren. 2023. SINE: SINgle Image Editing with Text-to-Image Diffusion Models. In *IEEE/CVF Conference on Computer Vision and Pattern Recognition (CVPR)*. 6027–6037.

[110] Minfeng Zhu, Pingbo Pan, Wei Chen, and Yi Yang. 2019. DM-GAN: Dynamic Memory Generative Adversarial Networks for Text-to-Image Synthesis. In *IEEE/CVF Conference on Computer Vision and Pattern Recognition (CVPR)*. 5802–5810.